New Journal of Physics
The open access journal at the forefront of physics
Deutsche Physikalische Gesellschaft DPG | IOP Institute of Physics

Neutrino cosmology and Planck

Julien Lesgourgues[1] **and Sergio Pastor**[2]

[1] Institut de Théorie des Phénomènes Physiques, EPFL, CH-1015 Lausanne, Switzerland CERN, Theory Division, CH-1211 Geneva 23, Switzerland LAPTh (CNRS-Université de Savoie), B.P. 110, F-74941 Annecy-le-Vieux Cedex, France
[2] Instituto de Física Corpuscular (CSIC-Universitat de València), c/ Catedrático José Beltrán, 2, E-46980 Paterna (Valencia), Spain
E-mail: Julien.Lesgourgues@cern.ch and Sergio.Pastor@ific.uv.es

Received 25 January 2014, revised 8 April 2014
Accepted for publication 22 April 2014
Published 5 June 2014

New Journal of Physics **16** (2014) 065002

doi:10.1088/1367-2630/16/6/065002

Abstract

Relic neutrinos play an important role in the evolution of the Universe, modifying some of the cosmological observables. We summarize the main aspects of cosmological neutrinos and describe how the precision of present cosmological data can be used to learn about neutrino properties. In particular, we discuss how cosmology provides information on the absolute scale of neutrino masses, complementary to beta decay and neutrinoless double-beta decay experiments. We explain why the combination of Planck temperature data with measurements of the baryon acoustic oscillation angular scale provides a strong bound on the sum of neutrino masses, 0.23 eV at the 95% confidence level, while the lensing potential spectrum and the cluster mass function measured by Planck are compatible with larger values. We also review the constraints from current data on other neutrino properties. Finally, we describe the very good perspectives from future cosmological measurements, which are expected to be sensitive to neutrino masses close to the minimum values guaranteed by flavour oscillations.

Keywords: neutrino masses, cosmology, dark matter

1. Introduction

The role of neutrinos in cosmology is one of the best examples of the very close ties that have developed between nuclear physics, particle physics, astrophysics and cosmology. Here we focus on the most interesting aspects related to the case of massive (and light) relic neutrinos, but many others that were left out can be found in specialized books [1] and reviews [2–7].

We begin with a description of the properties and evolution of the background of relic neutrinos that fill the Universe. The largest part of this paper is devoted to the impact of massive neutrinos on cosmological observables, which can be used to extract bounds on neutrino masses from present data, with emphasis on the results of the Planck satellite. Next, we review the implication of current cosmological data on other neutrino properties (relic density, leptonic asymmetry, extra sterile neutrino species). Finally, we discuss the sensitivities of future cosmological experiments to neutrino masses.

2. The cosmic neutrino background

The existence of a relic sea of neutrinos is a generic feature of the standard hot big bang model, in number only slightly below that of relic photons that constitute the cosmic microwave background (CMB). This cosmic neutrino background (CNB) has not been detected yet, but its presence is indirectly established by the accurate agreement between the calculated and observed primordial abundances of light elements, as well as from the analysis of the power spectrum of CMB anisotropies and other cosmological observables.

Produced at high temperatures by frequent weak interactions, flavour neutrinos ($\nu_{e,\mu,\tau}$) were kept in equilibrium until these processes became ineffective in the course of the expansion of the early Universe. While coupled to the rest of the primeval plasma (relativistic particles such as electrons, positrons and photons), neutrinos had a momentum spectrum with an equilibrium Fermi–Dirac form with temperature T,

$$f_{\rm eq}\left(p,\,T\right)=\left[\exp\left(\frac{p-\mu_\nu}{T}\right)+1\right]^{-1}, \tag{1}$$

which is just one example of the general case of particles in equilibrium (fermions or bosons, relativistic or non-relativistic), as shown e.g. in [8]. In the previous equation we have included a neutrino chemical potential μ_ν that would exist in the presence of a neutrino-antineutrino asymmetry, but it has been shown that, even if it exists, its contribution cannot be very relevant [9].

As the Universe cools, the weak interaction rate falls below the expansion rate and neutrinos decouple from the rest of the plasma. An estimate of the decoupling temperature $T_{\rm dec}$ can be found by equating the thermally averaged value of the weak interaction rate $\Gamma_\nu=\langle\sigma_\nu\, n_\nu\rangle$, where $\sigma_\nu\propto G_F^2$ is the cross section of the electron-neutrino processes with G_F the Fermi constant, and n_ν is the neutrino number density, with the expansion rate given by the Hubble parameter $H=(8\pi\rho/3M_P^2)^{1/2}$. Here $\rho\propto T^4$ is the total energy density, dominated by radiation, and $M_P=1/G^{1/2}$ is the Planck mass. If we approximate the numerical factors to unity, with $\Gamma_\nu\approx G_F^2\,T^5$ and $H\approx T^2/M_P$, we obtain the rough estimate $T_{\rm dec}\approx 1$ MeV. More accurate

calculations give slightly higher values of $T_{\rm dec}$ which are flavour dependent because electron neutrinos and antineutrinos are in closer contact with $e^{\pm}$, as shown e.g. in [2].

Although neutrino decoupling is not described by a unique $T_{\rm dec}$, it can be approximated as an instantaneous process. The standard picture of *instantaneous neutrino decoupling* is very simple (see e.g. [8, 10]) and reasonably accurate. In this approximation, the spectrum in equation (1) is preserved after decoupling, because both neutrino momenta and temperature redshift identically with the expansion of the Universe. In other words, the number density of non-interacting neutrinos remains constant in a comoving volume since decoupling. We will see later that neutrinos cannot possess masses much larger than 1 eV, so they were ultra-relativistic at decoupling. This is the reason why the momentum distribution in equation (1) does not depend on the neutrino masses, even after decoupling, i.e. there is no neutrino energy in the exponential of $f_{\rm eq}\left(p\right)$.

When calculating quantities related to relic neutrinos, one must consider the various possible degrees of freedom per flavour. If neutrinos are massless or Majorana particles, there are two degrees of freedom for each flavour, one for neutrinos (one negative helicity state) and one for antineutrinos (one positive helicity state). Instead, for Dirac neutrinos there are in principle twice more degrees of freedom, corresponding to the two helicity states. However, the extra degrees of freedom should be included in the computation only if they are populated and brought into equilibrium before neutrinos decouple. In practice, the Dirac neutrinos with the 'wrong-helicity' states do not interact with the plasma at MeV temperatures and have a vanishingly small density with respect to the usual left-handed neutrinos (unless neutrinos have masses close to the keV range, as explained in section 6.4 of [2], but this possibility is excluded). Thus the relic density of active neutrinos does not depend on their nature, either Dirac or Majorana particles.

Shortly after neutrino decoupling, the temperature drops below the electron mass, favouring $e^{\pm}$ annihilations into photons. If one assumes that this entropy transfer did not affect the neutrinos because they were already completely decoupled, it is easy to calculate the change in the photon temperature before any $e^{\pm}$ annihilation and after the $e^{\pm}$ pairs disappear by assuming entropy conservation of the electromagnetic plasma. The result, $T_\gamma^{\rm after}/T_\gamma^{\rm before} = (11/4)^{1/3} \simeq 1.40102$, is also the ratio between the temperatures of relic photons and neutrinos T_γ/T_ν. During the process of $e^{\pm}$ annihilations, T_γ decreases with the expansion less than the inverse of the scale factor a. Instead, the temperature of the decoupled neutrinos always falls as $1/a$.

It turns out that the processes of neutrino decoupling and $e^{\pm}$ annihilations are sufficiently close in time so that some relic interactions between $e^{\pm}$ and neutrinos exist. These relic processes are more efficient for larger neutrino energies, leading to non-thermal distortions in the neutrino spectra at the percent level and a slightly smaller increase of the comoving photon temperature, as noted in a series of works listed in [1, 2]. These changes modify the contribution of relativistic relic neutrinos to the total energy density which is taken into account using $N_{\rm eff} \simeq 3.046$ [11], as defined later in equation (6). In practice, these distortions only have small consequences on the evolution of cosmological perturbations, and for many purposes they can be safely ignored.

Any quantity related to relic neutrinos can be calculated after decoupling with the spectrum in equation (1) and T_ν. For instance, the number density per flavour is

$$n_\nu = \frac{3}{11}\, n_\gamma = \frac{6\zeta(3)}{11\pi^2}\, T_\gamma^3, \tag{2}$$

which leads to a present value of 113 neutrinos and antineutrinos of each flavour per cm^3. Instead, the energy density for massive neutrinos should in principle be calculated numerically, with two well-defined analytical limits,

$$\rho_\nu\left(m_\nu \ll T_\nu\right) = \frac{7\pi^2}{120}\left(\frac{4}{11}\right)^{4/3} T_\gamma^4, \qquad \rho_\nu\left(m_\nu \gg T_\nu\right) = m_\nu n_\nu. \tag{3}$$

Let us now discuss the evolution of the CNB after decoupling in the expanding Universe, which is described by the Friedmann–Robertson–Walker metric [10]

$$ds^2 = dt^2 - a\left(t\right)^2 \delta_{ij} dx^i dx^j, \tag{4}$$

where we assumed negligible spatial curvature. Here $a(t)$ is the scale factor usually normalized to unity now ($a\left(t_0\right) = 1$) and related to the redshift z as $a = 1/\left(1 + z\right)$. General relativity tells us the relation between the metric and the matter and energy via the Einstein equations, whose time–time component is the Friedmann equation

$$\left(\frac{\dot{a}}{a}\right)^2 = H^2 = \frac{8\pi G}{3}\rho = H_0^2 \frac{\rho}{\rho_\mathrm{c}^0}, \tag{5}$$

which gives the Hubble rate in terms of the total energy density ρ. At any time, the critical density ρ_c is defined as $\rho_\mathrm{c} = 3\,H^2/8\pi G$, with a current value $\rho_\mathrm{c}^0 = 1.8788 \times 10^{-29}\, h^2\ \mathrm{g\ cm}^{-3}$, where $h \equiv H_0/\left(100\ \mathrm{km\ s}^{-1}\ \mathrm{Mp\ c}^{-1}\right)$. The different contributions to the total energy density are $\rho = \rho_\gamma + \rho_\mathrm{cdm} + \rho_\mathrm{b} + \rho_\nu + \rho_\Lambda$, and the evolution of each component is given by the energy conservation law in an expanding Universe $\dot{\rho} = -\,3\,H\left(\rho + p\right)$, where p is the pressure. Thus the homogeneous density of photons ρ_γ scales like a^{-4}, that of non-relativistic matter (ρ_cdm for cold dark matter and ρ_b for baryons) like a^{-3}, and the cosmological constant density ρ_Λ is of course time-independent. Instead, the energy density of neutrinos contributes to the radiation density at early times, but they behave as matter after the non-relativistic transition.

The evolution of all densities is depicted in figure 1, starting at MeV temperatures until now. The density fractions $\Omega_i \equiv \rho_i/\rho_\mathrm{c}$ are shown in this figure, where it is easy to see which of the Universe components dominates, fixing its expansion rate: first, radiation in the form of photons and neutrinos (radiation domination); then matter, which can be CDM, baryons and massive neutrinos at late times (matter domination); and finally, the cosmological constant density takes over at low z (typically $z < 0.5$).

Massive neutrinos are the only known particles that present a late transition from radiation to matter, when their density is clearly enhanced (upper solid lines in figure 1). Obviously, the contribution of massive neutrinos to the energy density in the non-relativistic limit is a function of the mass (or the sum of all masses for which $m_i \gg T_\nu$), and the present value Ω_ν could be of order unity for eV masses (see section 4).

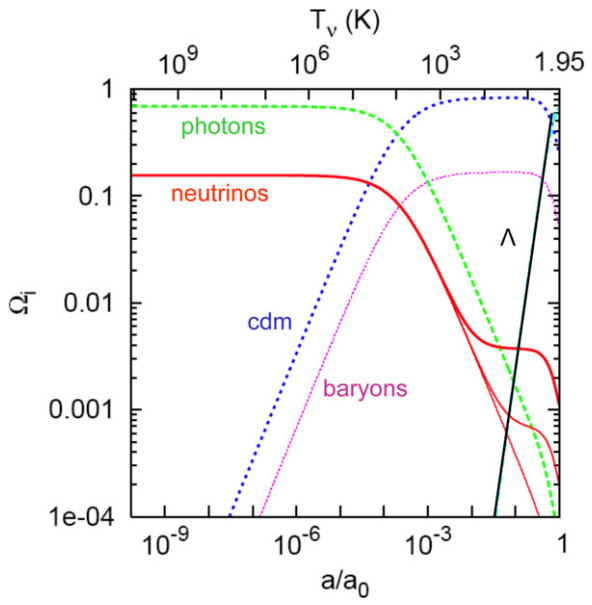

Figure 1. Evolution of the background energy densities in terms of the fractions Ω_i, from $T_\nu = 1$ MeV until now, for each component of a flat Universe with $h = 0.7$ and current density fractions $\Omega_\Lambda = 0.70$, $\Omega_\mathrm{b} = 0.05$ and $\Omega_\mathrm{cdm} = 1 - \Omega_\Lambda - \Omega_\mathrm{b} - \Omega_\nu$. The three neutrino masses are $m_1 = 0$, $m_2 = 0.009$ eV and $m_3 = 0.05$ eV.

3. Extra radiation and the effective number of neutrinos

Together with photons, in the standard case neutrinos fix the expansion rate while the Universe is dominated by radiation. Their contribution to the total radiation content can be parametrized in terms of the effective number of neutrinos N_eff, defined as

$$\rho_\mathrm{r} = \rho_\gamma + \rho_\nu = \left[1 + \frac{7}{8}\left(\frac{4}{11}\right)^{4/3} N_\mathrm{eff}\right] \rho_\gamma \,, \tag{6}$$

where we have normalized ρ_r to the photon energy density because its value today is known from the measurement of the CMB temperature. This equation is valid when neutrino decoupling is complete and holds as long as all neutrinos are relativistic.

We know that the number of light neutrinos sensitive to weak interactions (flavour or active neutrinos) equals three from the analysis of the invisible Z-boson width at LEP, $N_\nu = 2.9840 \pm 0.0082$ [12], and we saw in a previous section from the analysis of neutrino decoupling that they contribute as $N_\mathrm{eff} \simeq 3.046$. Any departure of N_eff from this last value would be due to non-standard neutrino features or to the contribution of other relativistic relics. For instance, the energy density of a hypothetical scalar particle ϕ in equilibrium with the same temperature as neutrinos would be $\rho_\phi = \left(\pi^2/30\right) T_\nu^4$, leading to a departure of N_eff from the standard value of 4/7. A detailed discussion of cosmological scenarios where N_eff is not fixed to three can be found in [1, 2, 13].

Relativistic particles, such as neutrinos, fix the expansion rate during big bang nucleosynthesis (BBN)[3], which in turn fixes the produced abundances of light elements, and in particular that of ^{4}He. Thus, the value of $N_{\rm eff}$ is constrained at BBN from the comparison of theoretical predictions and experimental data on the primordial abundances of light elements [14, 15]. This is why BBN gave the first allowed range of the number of neutrino species before accelerators. In a recent analysis of the BBN constraints on $N_{\rm eff}$ [16] (see the references therein for other analyses), the authors discuss a new and more conservative approach, motivated by growing concerns about the reliability of astrophysical determinations of primordial ^{4}He. According to [16], BBN limits the extra radiation to $\Delta N_{\rm eff} \leqslant 1$ at 95% C.L.

In addition, a value of $N_{\rm eff}$ different from the standard one would affect the CMB observables, as will be explained in section 7.1. We will see that the Planck satellite measurement is in very good agreement with both the standard prediction of $N_{\rm eff} \simeq 3.046$ and BBN results, in spite of a marginal preference for extra relativistic degrees of freedom (exacerbated if astrophysical measurements of H_0 are included).

4. Massive neutrinos as dark matter

Nowadays the existence of dark matter (DM), the dominant non-baryonic component of the matter density in the Universe, is well established. *A priori*, massive neutrinos are excellent DM candidates, in particular because we are certain that they exist, in contrast with other candidate particles. Their energy density in units of the critical value is

$$\Omega_\nu = \frac{\rho_\nu}{\rho_{\rm c}^0} = \frac{\sum_i m_i}{93.14\, h^2 {\rm eV}}. \tag{7}$$

Here $\sum_i m_i$ includes all masses of the neutrino states which are non-relativistic today. It is also useful to define the neutrino density fraction with respect to the matter density

$$f_\nu \equiv \frac{\rho_\nu}{\left(\rho_{\rm cdm} + \rho_{\rm b} + \rho_\nu\right)} = \frac{\Omega_\nu}{\Omega_{\rm m}}. \tag{8}$$

In order to find the contribution of relic neutrinos to the present values of Ω_ν or f_ν, we should consider which neutrino masses are allowed by non-cosmological data. Oscillation experiments measure $\Delta m^2_{21} = m_2^2 - m_1^2$ and $\Delta m^2_{31} = m_3^2 - m_1^2$, the relevant differences of squared neutrino masses for solar and atmospheric neutrinos, respectively. As a reference, we take the 3σ ranges of mixing parameters from [17] (see also [18, 19]),

$$s^2_{12} = 0.32 \pm 0.05 \quad s^2_{23} \in \left[0.36,\, 0.68\right] \left(\left[0.37,\, 0.67\right]\right) \quad s^2_{13} = 0.0246^{+0.0084}_{-0.0076} \ \left(0.025 \pm 0.008\right)$$
$$\Delta m^2_{21}\left(10^{-5}\ {\rm eV}^2\right) = 7.62^{+0.58}_{-0.50} \qquad \Delta m^2_{31}\left(10^{-3}\ {\rm eV}^2\right) = 2.55^{+0.19}_{-0.24} \ \left(-2.43^{+0.21}_{-0.22}\right). \tag{9}$$

Here $s^2_{ij} = \sin^2\theta_{ij}$, where θ_{ij} ($ij = 12$, 23 or 13) are the three mixing angles. Unfortunately, oscillation experiments are insensitive to the absolute scale of neutrino masses, because the

[3] In addition, BBN is the last cosmological epoch sensitive to neutrino flavour, because electron neutrinos and antineutrinos play a direct role in the weak processes.

knowledge of $\Delta m^2_{21} > 0$ and $|\Delta m^2_{31}|$ leads to the two possible schemes shown in figure 1 of [4], but leaves one neutrino mass unconstrained. These two schemes are known as normal (NH, $\Delta m^2_{31} > 0$) and inverted (IH, $\Delta m^2_{31} < 0$) mass hierarchies. In the above equation the values in parentheses correspond to the IH, otherwise the allowed regions are the same for both hierarchies. For small values of the lightest neutrino mass m_0, i.e. m_1 (m_3) for NH (IH), the mass states follow a hierarchical scenario, while for masses much larger than the differences all neutrinos share in practice the same mass (degenerate region). In general, the relation between the individual masses and the total neutrino mass can be found numerically.

There are two types of laboratory experiments searching for the absolute scale of neutrino masses, a crucial piece of information for constructing models of neutrino masses and mixings. The neutrinoless double beta decay $(Z, A) \rightarrow (Z + 2, A) + 2e^-$ (in short $0\nu 2\beta$) is a rare nuclear processes where lepton number is violated and whose observation would mean that neutrinos are Majorana particles. If the $0\nu 2\beta$ process is mediated by a light neutrino, the results from neutrinoless double beta decay experiments are converted into an upper bound or a measurement of the effective mass

$$m_{\beta\beta} = \left| c_{12}^2 c_{13}^2 \, m_1 + s_{12}^2 c_{13}^2 \, m_2 \, e^{i\phi_2} + s_{13}^2 \, m_3 \, e^{i\phi_1} \right|, \tag{10}$$

where $\phi_{1,2}$ are two Majorana phases that appear in lepton-number-violating processes. An important issue for $0\nu 2\beta$ results is related to the uncertainties on the corresponding nuclear matrix elements. For more details and the current experimental results, see [20].

Beta decay experiments, which involve only the kinematics of electrons, are in principle the best strategy for measuring directly the neutrino mass [21]. The current limits from tritium beta decay apply only to the range of degenerate neutrino masses, so that $m_\beta \simeq m_0$, where

$$m_\beta = \left(c_{12}^2 c_{13}^2 \, m_1^2 + s_{12}^2 c_{13}^2 \, m_2^2 + s_{13}^2 \, m_3^2 \right)^{1/2}, \tag{11}$$

is the relevant parameter for beta decay experiments. The bound at 95% CL is $m_0 < 2.05 - 2.3$ eV from the Troitsk and Mainz experiments, respectively. This value is expected to be improved by the KATRIN project to reach a discovery potential for $0.3 - 0.35$ eV masses (or a sensitivity of 0.2 eV at 90% CL). Taking into account this upper bound and the minimal values of the total neutrino mass in the normal (inverted) hierarchy, the sum of neutrino masses $M_\nu \equiv \sum_i m_i$ is restricted to the approximate range

$$0.06 \ (0.1) \text{ eV} \lesssim M_\nu \lesssim 6 \text{ eV} \tag{12}$$

As we discuss in the next sections, cosmology is at first order sensitive to the total neutrino mass if all states have the same number density, providing information on m_0 but blind to neutrino mixing angles or possible CP violating phases. Thus cosmological results are complementary to terrestrial experiments. The interested reader can find the allowed regions in the parameter space defined by any pair of parameters $(M_\nu, m_{\beta\beta}, m_\beta)$ in [22–24]. The two cases involving M_ν are shown in figure 2.

Now we can find the possible present values of Ω_ν in agreement the approximate bounds of equation (12). Note that even if the three neutrinos are non-degenerate in mass, equation (7) can be safely applied, because we know from neutrino oscillation data that at least two of the neutrino states are non-relativistic today, because both $|\Delta m^2_{31}|^{1/2} \simeq 0.05$ eV and

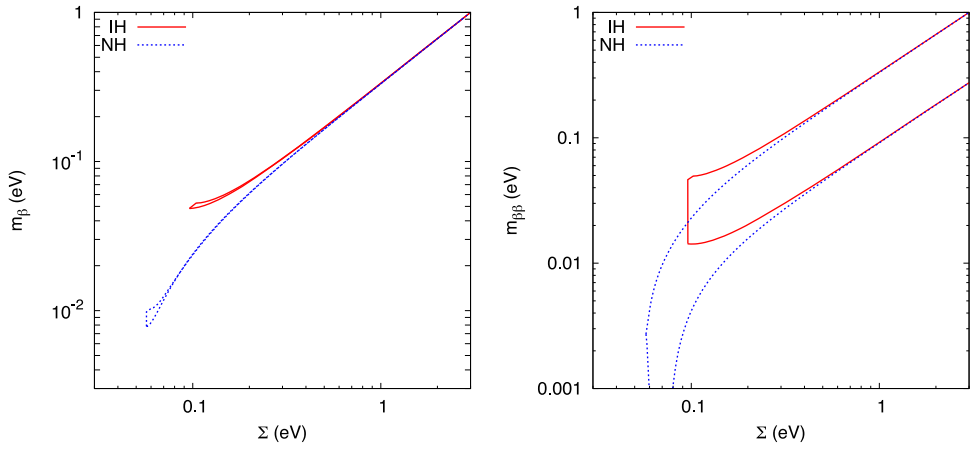

Figure 2. Allowed regions by oscillation data at the 3σ level (equation (9)) of the three main observables sensitive to the absolute scale of neutrino masses. We show the regions in the planes $m_\beta - \Sigma$ and $m_{\beta\beta} - \Sigma$, where Σ is the sum of neutrino masses. Blue dotted (red solid) regions correspond to normal (inverted) hierarchy.

$\left(\Delta m^2_{21}\right)^{1/2} \simeq 0.009$ eV are higher than the temperature $T_\nu \simeq 1.96$ K $\simeq 1.7 \times 10^{-4}$ eV. If the third neutrino state is very light and still relativistic, its relative contribution to Ω_ν is negligible and equation (7) remains an excellent approximation of the total density. One finds that Ω_ν is restricted to the approximate range

$$0.0013 \ \left(0.0022\right) \lesssim \Omega_\nu \lesssim 0.13, \tag{13}$$

where we already included that $h \approx 0.7$. This applies only to the standard case of three light active neutrinos, while in general a cosmological upper bound on Ω_ν has been used since the 1970s to constrain the possible values of neutrino masses. For instance, if we demand that neutrinos should not be heavy enough to overclose the Universe ($\Omega_\nu < 1$), we obtain an upper bound $M_\nu \lesssim 45$ eV (again fixing $h = 0.7$). Moreover, from present analyses of cosmological data we know that the approximate contribution of matter is $\Omega_{\rm m} \simeq 0.3$, and the neutrino masses should obey the stronger bound $M_\nu \lesssim 15$ eV. Thus, with this simple argument one obtains a bound which is roughly only a factor two worse than the bound from tritium beta decay, but of course with the caveats that apply to any cosmological analysis. In the three-neutrino case, these bounds should be understood in terms of $m_0 = M_\nu/3$.

Dark matter particles with a large velocity dispersion, such as that of neutrinos, are called hot dark matter (HDM). The role of neutrinos as HDM particles has been widely discussed since the 1970s (see e.g. the historical review [25]). It was realized in the mid-1980s that HDM affects the evolution of cosmological perturbations in a particular way: it erases the density contrasts on wavelengths smaller than a mass-dependent free-streaming scale. In a universe dominated by HDM, this suppression contradicts various observations. For instance, large objects such as superclusters of galaxies form first, while smaller structures such as clusters and galaxies form via a fragmentation process. This top-down scenario is at odds with the fact that galaxies seem older than clusters.

Given the failure of HDM-dominated scenarios, the attention then turned to cold dark matter (CDM) candidates, i.e. particles which were non-relativistic at the epoch when the

universe became matter-dominated, which provided a better agreement with observations. Still in the mid-1990s it appeared that a small mixture of HDM in a universe dominated by CDM fitted better the observational data on density fluctuations at small scales than a pure CDM model. However, within the presently favoured ΛCDM model dominated at late times by a cosmological constant (or some form of dark energy) there is no need for a significant contribution of HDM. Instead, one can use the available cosmological data to find how large the neutrino contribution can be, as we will see later.

Before concluding this section, we would like to mention the case of a sterile neutrino with a mass of the order of a few keVs and a very small mixing with the flavour neutrinos. Such 'heavy' neutrinos could be produced by active-sterile oscillations, but not fully thermalized, so that they could replace the usual CDM component. But due to their large thermal velocity (slightly smaller than that of active neutrinos), they would behave as warm dark matter and erase small-scale cosmological structures. Their mass can be bounded from below using Lyman-α forest data from quasar spectra, and from above using x-ray observations. The viability of this scenario was reviewed in [26].

5. Effects of neutrino masses on cosmology

Here we briefly describe the main cosmological observables, and their sensitivity to neutrino masses. A more detailed discussion of the effects of massive neutrinos on the evolution of cosmological perturbations can be found in sections 5.3.3 and 6.1.4 of [1].

5.1. Brief description of cosmological observables

Although there exist many different types of cosmological measurements, here we will restrict the discussion to those that are at present the more important for obtaining an upper bound or eventually a measurement of neutrino masses.

First of all, we have the CMB temperature anisotropy power spectrum, defined as the angular two-point correlation function of CMB maps $\delta T/\bar{T}\left(\hat{n}\right)$ ($\hat{n}$ being a direction in the sky). This function is usually expanded in Legendre multipoles

$$\left\langle \frac{\delta T}{\bar{T}}\left(\hat{n}\right)\frac{\delta T}{\bar{T}}\left(\hat{n}'\right)\right\rangle = \sum_{l=0}^{\infty}\frac{\left(2\,l+1\right)}{4\pi}\,C_l\,P_l\left(\hat{n}\cdot\hat{n}'\right), \tag{14}$$

where $P_l\left(x\right)$ are the Legendre polynomials. For Gaussian fluctuations, all the information is encoded in the multipoles C_l which probe correlations on angular scales $\theta = \pi/l$. There exists interesting complementary information to the temperature power spectrum if the CMB polarization is measured, and currently we have some less precise data on the temperature × E-polarization (TE) correlation function and the E-polarization self-correlation spectrum (EE).

The current large scale structure (LSS) of the Universe is probed by the matter power spectrum at a given time or redshift z. It is defined as the two-point correlation function of non-relativistic matter fluctuations in Fourier space

$$P\left(k,\,z\right) = \left\langle \left|\delta_{\rm m}\left(k,\,z\right)\right|^2\right\rangle, \tag{15}$$

where $\delta_{\rm m} = \delta\rho_{\rm m}/\bar{\rho}_{\rm m}$. Usually $P(k)$ refers to the matter power spectrum evaluated today (at $z = 0$). In the case of several fluids (e.g. CDM, baryons and non-relativistic neutrinos), the total matter

perturbation can be expanded as $\delta_{\rm m} = \sum_i \bar{\rho}_i \, \delta_i / \sum_i \bar{\rho}_i$. Because the energy density is related to the mass density of non-relativistic matter through $E = mc^2$, $\delta_{\rm m}$ represents indifferently the energy or mass power spectrum. The shape of the matter power spectrum is affected in a scale-dependent way by the free-streaming caused by small neutrino masses of O(eV) and thus it is the key observable for constraining m_ν with cosmological methods.

5.2. Neutrino free-streaming

After thermal decoupling, relic neutrinos constitute a collisionless fluid, where the individual particles free-stream with a characteristic velocity that, on average, is the thermal velocity $v_{\rm th}$. It is possible to define a horizon as the typical distance on which particles travel between time t_i and t. When the Universe was dominated by radiation or matter $t \gg t_i$, this horizon is, as usual, asymptotically equal to $v_{\rm th}/H$, up to a numerical factor of order one. Similar to the definition of the Jeans length (see section 4.4 in [4]), we can define the neutrino free-streaming wavenumber

$$k_{FS}(t) = \left(\frac{4\pi G \bar{\rho}(t) a^2(t)}{v_{\rm th}^2(t)} \right)^{1/2}. \tag{16}$$

As long as neutrinos are relativistic, they travel at the speed of light, and their free-streaming length is simply equal to the Hubble radius. When they become non-relativistic, their thermal velocity decays like

$$v_{\rm th} \equiv \frac{\langle p \rangle}{m} \simeq \frac{3.15 T_\nu}{m} = \frac{3.15 T_\nu^0}{m} \left(\frac{a_0}{a} \right) \simeq 158 (1+z) \left(\frac{1\ {\rm eV}}{m} \right) {\rm km\ s^{-1}}, \tag{17}$$

where we used for the present neutrino temperature $T_\nu^0 \simeq (4/11)^{1/3} T_\gamma^0$ and $T_\gamma^0 \simeq 2.726$ K. This gives for the free-streaming wavenumber during matter or Λ domination

$$k_{FS}(t) = 0.8 \frac{\sqrt{\Omega_\Lambda + \Omega_m (1+z)^3}}{(1+z)^2} \left(\frac{m}{1\ {\rm eV}} \right) h\ {\rm Mp\ c^{-1}}, \tag{18}$$

where Ω_Λ and Ω_m are the cosmological constant and matter density fractions, respectively, evaluated today. After the non-relativistic transition and during matter domination, the free-streaming length continues to increase, but only like $(aH)^{-1} \propto t^{1/3}$, i.e. more slowly than the scale factor $a \propto t^{2/3}$. Therefore, the comoving free-streaming length λ_{FS}/a actually decreases like $\left(a^2 H\right)^{-1} \propto t^{-1/3}$. As a consequence, for neutrinos becoming non-relativistic during matter domination, the comoving free-streaming wavenumber passes through a minimum $k_{\rm nr}$ at the time of the transition, i.e. when $m = \langle p \rangle = 3.15 T_\nu$ and $a_0/a = (1+z) = 2.0 \times 10^3 (m/1\ {\rm eV})$. This minimum value is found to be

$$k_{\rm nr} \simeq 0.018\ \Omega_{\rm m}^{1/2} \left(\frac{m}{1\ {\rm eV}} \right)^{1/2} h\ {\rm Mp\ c^{-1}}. \tag{19}$$

The physical effect of free-streaming is to damp small-scale neutrino density fluctuations: neutrinos cannot be confined into (or kept outside of) regions smaller than the free-streaming length, because their velocity is greater than the escape velocity from gravitational potential

wells on those scales. Instead, on scales much larger than the free-streaming scale, the neutrino velocity can be effectively considered as vanishing, and after the non-relativistic transition the neutrino perturbations behave like CDM perturbations. In particular, modes with $k < k_{\rm nr}$ are never affected by free-streaming and evolve as if in a pure ΛCDM model.

5.3. Impact of massive neutrinos on the matter power spectrum

The small initial cosmological perturbations evolve within the linear regime at early times. During matter domination, the smallest cosmological scales start evolving non-linearily, leading to the formation of the structures we see today. In the recent Universe, the largest observable scales are still related to the linear evolution, while other scales can only be understood using non-linear N-body simulations. We will not review here all the details of this complicated evolution (see [1, 4, 6] and references therein), but we will emphasize the main effects caused by massive neutrinos on linear scales in the framework of the standard cosmological scenario: a Λ mixed dark matter (ΛMDM) model, where 'mixed' refers to the inclusion of some HDM component.

On large scales (i.e. on wave-numbers smaller than the value $k_{\rm nr}$ defined in the previous subsection), neutrino free-streaming can be ignored, and neutrino perturbations are indistinguishable from CDM perturbations. On those scales, the matter power spectrum $P\left(k,\, z\right)$ can be shown to depend only on the matter density fraction today (including neutrinos), $\Omega_{\rm m}$, and on the primordial perturbation spectrum. If the neutrino mass is varied with $\Omega_{\rm m}$ fixed, the large-scale power spectrum remains invariant.

However, the small-scale matter power spectrum $P\left(k \geqslant k_{\rm nr}\right)$ is reduced in the presence of massive neutrinos for at least two reasons: by the absence of neutrino perturbations in the total matter power spectrum, and by a slower growth rate of CDM/baryon perturbations at late times. The third effect has the largest amplitude. At low redshift $z \simeq 0$, the step-like suppression of $P(k)$ starts at $k \geqslant k_{\rm nr}$ and saturates at $k \sim 1\, h$/Mpc with a constant amplitude $\Delta P\left(k\right)/P\left(k\right) \simeq -8 f_\nu$. This result was obtained by fitting numerical simulations [27], but a more accurate approximation can be derived analytically [1, 4]. The full matter power spectrum can be calculated at any time and scale by Boltzmann codes, such as CAMB [28] or CLASS [29], that solve numerically the evolution of the cosmological perturbations. The step-like suppression of the matter power spectrum induced by various values of f_ν is shown in figure 3.

On small scales and at late times, matter density perturbations enter into the regime of non-linear clustering. The neutrino mass impact on the non-linear matter power spectrum is now modeled with rather good precision, at least within one decade above $k_{\rm max}$ in wave-number space [30–32]. It appears that the step-like suppression is enhanced by non-linear effects up to roughly $\Delta P\left(k\right)/P\left(k\right) \simeq -10 f_\nu$ (at redshift zero and $k \sim 1\ h\ {\rm Mpc}^{-1}$), and is reduced above this scale. Hence, non-linear corrections render the neutrino mass effect even more characteristic than in the linear theory, and may help to increase the sensitivity of future experiments (see also [33–35] for the effect of neutrino masses on even smaller scales).

Until this point, we reduced the neutrino mass effect to that of f_ν or M_ν. In principle, the mass splitting between the three different families for a common total mass is visible in $P(k)$. The time at which each species becomes non-relativistic depends on individual masses m_i. Hence, both the scale of the step-like suppression induced by *each* neutrino and the amount of

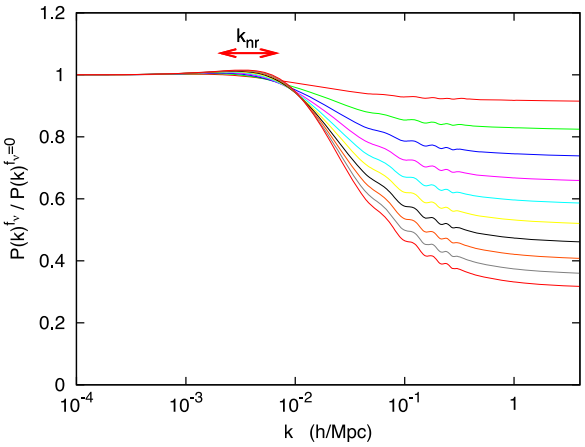

Figure 3. Ratio of the matter power spectrum including three degenerate massive neutrinos with density fraction f_ν to that with three massless neutrinos. The parameters $(\omega_{\rm m}, \Omega_\Lambda) = (0.147, 0.70)$ are kept fixed, and from top to bottom the curves correspond to $f_\nu = 0.01, 0.02, 0.03, \ldots, 0.10$. The individual masses m_ν range from 0.046 to 0.46 eV, and the scale $k_{\rm nr}$ from $2.1 \times 10^{-3} h$ Mp c^{-1} to $6.7 \times 10^{-3} h$ Mp c^{-1} as shown on the top of the figure. From [4].

suppression in the small-scale power spectrum have a small dependence on individual masses. The differences between the power spectrum of various models with the same total mass and different mass splittings was computed numerically in [36] for the linear spectrum, and [32] for the non-linear spectrum. At the moment, it seems that even the most ambitious future surveys will not be able to distinguish these mass splitting effects with a reasonable significance [37, 38].

5.4. Impact of massive neutrinos on the CMB anisotropy spectrum

For masses smaller than 0.6 eV, neutrinos are still relativistic at the time of photon decoupling, and their mass cannot impact the evolution of CMB perturbations. Therefore, the effect of the mass can only appear at two levels: that of the background evolution, and that of secondary anisotropies (related to the behaviour of photon perturbations after decoupling: integrated Sachs-Wolfe (ISW) effect, weak lensing by large scale structure, etc).

Let us first review the background effects of massive neutrinos on the CMB. Because the temperature and polarization spectrum shape is the result of several intricate effects, one cannot discuss the neutrino mass impact without specifying which other parameters are kept fixed. Neutrinos with a mass in the range from 10^{-3} eV to 1 eV should be counted as radiation at the time of equality, and as non-relativistic matter today; the total non-relativistic density, parametrized by $\omega_{\rm m} = \Omega_{\rm m} h^2$, depends on the total neutrino mass $M_\nu = \sum_i m_i$. Hence, when M_ν is varied, there must be a variation either in the redshift of matter-to-radiation equality $z_{\rm eq}$, or in the matter density today $\omega_{\rm m}$.

This can potentially impact the CMB in three ways. A shift in the redshift of equality affects the position and amplitude of the peaks. A change in the non-relativistic matter density at late times can impact both the angular diameter distance to the last scattering surface $d_A\left(z_{\rm dec}\right)$,

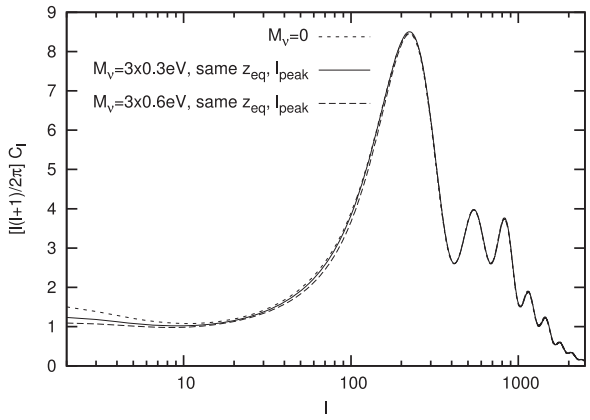

Figure 4. CMB temperature spectrum with different neutrino masses. Some of the parameters of the Λ MDM model have been varied together with M_ν in order to keep fixed the redshift of equality and the angular diameter distance to last scattering.

controlling the overall position of CMB spectrum features in multipole space, and the slope of the low-l tail of the CMB spectrum, due to the late ISW effect. Out of these three effects (changes in $z_{\rm eq}$, in d_A and in the late ISW), only two can be cancelled by a simultaneous variation of the total neutrino mass and of other free parameters in the ΛMDM model. Hence, the CMB spectrum is sensitive to the background effect of the total neutrino mass. In practice, however, the late ISW effect is difficult to measure due to cosmic variance, and CMB data alone cannot provide useful information on sub-eV neutrino masses. If one considers extensions of the ΛMDM, this becomes even more clear: by playing with the spatial curvature, one can neutralize all three effects simultaneously. But as soon as CMB data is used in combination with other background cosmology observations (constraining for instance the Hubble parameter, the cosmological constant value or the baryon acoustic oscillation (BAO) scale), some bounds can be derived on M_ν.

There exists another effect of massive neutrinos on the CMB at the level of secondary anisotropies: when neutrinos become non-relativistic, they reduce the time variation of the gravitational potential inside the Hubble radius. This affects the photon temperature through the early ISW effect, and leads to a depletion in the temperature spectrum of the order of $\left(\Delta C_l/C_l\right) \sim -\left(M_\nu/0.3\ \text{eV}\right)\%$ on multipoles $20 < l < 500$, with a dependence of the maximum depletion scale on individual masses m_i [1, 39]. This effect is roughly 30 times smaller than the depletion in the small-scale matter power spectrum, $\Delta P\left(k\right)/P\left(k\right) \sim -\left(M_\nu/0.01\ \text{eV}\right)\%$.

We show in figure 4 the effect on the CMB temperature spectrum of increasing the neutrino mass while keeping $z_{\rm eq}$ and d_A fixed: the only observed differences are then for $2 < l < 50$ (late ISW effect due to neutrino background evolution) and for $50 < l < 200$ (early ISW effect due to neutrino perturbations).

We conclude that the CMB alone is not a very powerful tool for constraining sub-eV neutrino masses, and should be used in combination with homogeneous cosmology constraints and/or measurements of the LSS power spectrum, for instance from galaxy clustering, galaxy lensing or CMB lensing.

6. Current bounds on neutrino masses

In this section, we review the neutrino mass bounds that can be derived from current cosmological data. Note that the confidence limits in the next subsections are all based on the Bayesian inference method, and are given at the 95% confidence level after marginalization over all free cosmological parameters. We refer the reader to section 5.1 of [4] for a detailed discussion on this statistical method.

6.1. CMB anisotropy bounds

The best measurement of CMB temperature anisotropies comes from the first release of the Planck satellite [40, 41], which significantly improved over the nine-year data of WMAP [42] on large angular scales, and over ground-based or balloon-borne (ACT, SPT, …) on small scales. Moreover, the Planck temperature data offers the advantage of covering all relevant angular scales with a single experiment, hence avoiding relative calibration issues between different data sets. The publication of polarization data has been postponed to the next Planck release. In the meantime, Planck temperature data is usually analyzed together with the $l \leqslant 23$ multipoles of WMAP E-type polarization (referred to later as WP), in order to remove degeneracies between the optical depth to reionization and other parameters. Moreover, Planck temperature data is used only up to the multipole $l = 2500$: for larger ls, it is better to use higher-resolution experiments (ACT, SPT), limited to $l > 2500$ to avoid any overlap, and called usually 'highL'. Note that including information on temperature at $l > 2500$ can be useful for separating the various foregrounds from the CMB signal, but it has a very minor impact on cosmological parameters, which are well constrained by the Planck + WP data alone [41].

Assuming the minimal ΛCDM model with six free parameters, and promoting the total neutrino mass M_ν as a seventh free parameter, one gets $M_\nu < 0.66$ eV (95%; Planck + WP + highL) [41]. As explained in section 5.4, this bound comes mainly from two physical effects: the early-ISW-induced dip at intermediate ls, and the lensing effect causing a smoothing of the power spectrum at higher ls. To show that the latter effect is important, one can treat the amplitude of the lensing potential spectrum as a free parameter (while in reality, its value is fully predicted by the underlying cosmological model). This is equivalent to partially removing the piece of information coming from the lensing of the last scattering surface. Then, the mass bound degrades by 63%.

Assuming an extended underlying cosmological model, the mass bound gets weaker. This is true especially if one allows for non-zero spatial curvature in the universe: the bound then degrades to $M_\nu < 0.98$ eV (95%; Planck + WP + highL). However, when the density of extra relativistic relics is promoted as a new free parameter, the bound on M_ν does not change significantly, showing that the current CMB data is able to resolve the degeneracy between M_ν and $N_{\rm eff}$ that used to exist when using older data sets.

6.2. Adding information on the cosmological expansion

The measurement of CMB anisotropies can be complemented by some data on the cosmological expansion at low redshift ($z < 2$). The recent expansion history can be inferred from the luminosity of type-Ia supernovae, from the angular scale of baryon acoustic

oscillations (BAO) reconstructed from the galaxy power spectrum at various redshifts, or from direct measurements of the current expansion rate H_0 through nearby cepheids and supernovae.

These measurements are very useful probes of neutrino masses, not directly but indirectly. Indeed, we have seen in section 5.4 that if the neutrino mass is varied at the same time as parameters controlling the late cosmological evolution (like Ω_Λ or Ω_k in a non-flat universe), most characteristic quantities affecting the shape of the CMB spectrum can be kept constant, including the angular scale of the first acoustic peak. Then, the effect of M_ν reduces to an irrelevant late ISW effect, plus the early ISW and lensing effects discussed above. But if instead these parameters are measured directly and constrained independently, the degeneracy is removed, and varying M_ν will also change the scale of the first peak. In that way, the CMB is very sensitive to M_ν, since the peak scale is the quantity best constrained by CMB observations.

The problem is that as long as one assumes a minimal ΛCDM model, the combination of CMB data with either BAO, H_0 or supernovae data reveals small tensions (roughly at the 2-σ level). This could mean either that some data sets have slightly underestimated systematics, or that something is not correct in the assumed underlying cosmological model. The main tension is between Planck + WP and HST measurements of H_0, giving respectively $H_0 = 67.3 \pm 2.54$ km s^{-1} Mpc^{-1}(95%; Planck + WP) and $H_0 = 73.8 \pm 4.8$ km s^{-1} Mpc^{-1}(95%; HST) [43]. BAO data are more consistent with Planck than with HST and exacerbate the tension, giving $H_0 = 67.8 \pm 1.5$ km s^{-1} Mpc^{-1}(95%; Planck + WP + BAO). Note that direct H_0 measurements probe the local value of the expansion parameter, while BAO and CMB data measure the expansion rate averaged over very large scales. However, in the standard cosmological model, the local and global H_0 are expected to differ by a tiny amount, so the tension cannot be explained in that way [44]. Promoting the total neutrino mass as a seventh free parameter does *not* release the tension either, since for the ΛCDM $+M_\nu$ model one finds $H_0 = 67.7 \pm 1.8$ km s^{-1} Mpc^{-1}(95%; Planck + WP + BAO) [41].

The neutrino mass bound also depends on which data is used. For CMB+BAO, one gets $M_\nu < 0.23$ eV (95%; Planck + WP + highL + BAO), while for CMB+HST one gets a stronger bound $M_\nu < 0.18$ eV (95%; Planck+WP+highL+BAO), and for CMB + supernovae the result is slightly looser, $M_\nu < 0.25$ eV (95%; Planck+WP+highL+SNLS) [41] (some of these numbers are not given in the Planck paper, but in the publicly released grid of bounds available at the ESA website[4]). If one takes the conservative point of view that the BAO data is the least likely to be affected by systematics because it is a pure geometrical measurement of an angle in the sky, one should mainly remember the first of these bounds (0.23 eV). This is already a very spectacular result, only a factor four higher than the minimum allowed value $M_\nu \sim 0.06$ eV.

6.3. Adding information on large scale structure

Large scale structure can be probed by Planck itself in several ways, using lensing extraction, foregrounds or spectral distorsions.

Among these probes, the most robust is expected to be lensing extraction, because it reconstructs the matter power spectrum mainly in the linear regime. Weak lensing of CMB

[4] http://sciops.esa.int/wikiSI/planckpla/ in section 6.9.

photons by large scale structure leads to a distortion of the CMB maps, and creates correlations in the observed map between multipoles on different scales (unlike in a pure Gaussian map). The lensing extraction technique consists of using these correlations in order to reconstruct the lensing field. In the same way, one can compute the lensing power spectrum, and get indications on the matter power spectrum over a range of scales and redshifts (typically, $1 < z < 3$) [45]. CMB lensing extraction was previously advocated as a way to improve the Planck error bar on the total neutrino mass by a factor two [46]. This cannot happen if the two data sets (anisotropy spectrum and extracted lensing spectrum) pull the results in opposite directions. Unfortunately, this is exactly what happens with the first Planck data release. We have seen that the Planck temperature spectrum puts strong limits on the mass. Instead, the extracted lensing spectrum has a marginal preference for a non-zero M_ν, because the step-like suppression induced by neutrino masses in the lensing spectrum gives a better fit. As a result, the bound gets looser when including lensing extraction: $M_\nu < 0.84$ eV (95%; Planck+WP+highL+lensing) or $M_\nu < 0.25$ eV (95%; Planck+WP+BAO+lensing). It will be interesting to see how these bounds will evolve in the next couple of years, with better data and better control over systematics in the lensing extraction process. The preference for a non-zero neutrino mass in the lensing data could then go away. Instead, there is still a possibility that lensing data correctly prefers $M_\nu > 0$, while some systematics in Planck data (for instance, in the low-l likelihood) artificially disfavour $M_\nu \neq 0$.

Spectral distortions of CMB maps caused by the Sunyaev–Zel'dovitch (SZ) effect allow the construction of a map of galaxy clusters. The distortions provide information on the position and redshift of the clusters, and even allow an estimatation of their mass up to some bias factor. The data can be used to make a histogram of the number of clusters as a function of redshift, or the mass of clusters as a function of redshift. These histograms can be compared to the predictions of structure formation theory (in the mildly non-linear regime). They give another handle on the underlying matter power spectrum, and hence on neutrino masses.

The situation with Planck SZ clusters is similar to the situation with lensing: the cluster data prefers a non-zero neutrino mass, unless the bias is assumed to take extreme value, that would normally be excluded by theoretical arguments. [47] gives a combined CMB + SZ cluster result preferring a non-zero neutrino mass at the 2.5σ level, $M_\nu = 0.22 \pm 0.18$ eV (95%; Planck+WP+BAO+SZ). [48] shows how the bounds depend on several assumptions made in the SZ cluster analysis. A similar trend exists with essentially all other data on the cluster mass function. The conclusion is that something remains to be understood: either systematics are underestimated in measurements of the cluster mass function, or the Planck temperature data has some incorrect feature pushing down the neutrino masses (so far, the former assumption sounds more plausible).

The CMB data can be combined with many other probes of large scale structure (galaxy spectrum, flux spectrum of Lyman-α forests in quasars, weak lensing surveys). Until now, these other data sets tended to be less constraining than those discussed here[5].

[5] Except for a recent measurement of the amplitude of the matter power spectrum, based on the BOSS galaxy redshift survey, which leads to a preference for a non-zero neutrino mass roughly at the 3-σ level [49].

7. Other neutrino properties

7.1. Neutrino density, non-thermal distortions and leptonic asymmetry

Previous estimates of the total neutrino mass rely on the standard neutrino decoupling model, leading to a neutrino density corresponding to $N_{\rm eff} = 3.046$ as long as neutrinos are relativistic. This model could be incorrect, or missing some physical ingredients. Hence neutrinos could in principle have a different density, coming from a different neutrino-to-photon temperature ratio, or from non-thermal distortions. For instance, this would be the case if some exotic particles would decay after neutrino decoupling, either producing extra relic neutrinos, or reheating the thermal bath.

Another possible reason leading to a larger $N_{\rm eff}$ would be the production of a very large neutrino-antineutrino asymmetry in the early Universe. In that case, the phase-space distribution of neutrinos at CMB times depends on the initial leptonic asymmetry of each family, and on the efficiency of neutrino oscillations in the early Universe; in any case, a leptonic asymmetry produced at early times would tend to enhance the total neutrino density at late times.

If neutrinos were massless, all the effects described above (over- or under-production of neutrinos, non-thermal distortions, leptonic asymmetry) would entirely be described by the value of $N_{\rm eff}$, because the equations of evolution of cosmological perturbations in the neutrino sector could be integrated over momentum. When neutrino masses are taken into account, this is no longer true. In that case, $N_{\rm eff}$ explicitly refers to the radiation density at early times, before the non-relativistic transition of neutrinos. Still, as long as individual neutrino masses are not too large, it is useful to analyze cosmological models with free $N_{\rm eff}$ and M_ν set in first approximation to its minimal value (0.06 eV), or with $N_{\rm eff}$ and M_ν both promoted as free parameters, with an arbitrary mass splitting. To be very rigorous, each model would require an individual analysis, but in fairly good approximation, their properties are well accounted by the two parameters $N_{\rm eff}$ and M_ν. This is no longer true when individual neutrino masses can be large (of the order of one or several electron-volts), as assumed in section 7.3 on massive sterile neutrinos.

Hence it is crucial to measure $N_{\rm eff}$ in order to check whether we correctly understand neutrino cosmology. However, if a value of $N_{\rm eff}$ larger than three was measured in CMB or LSS data, we still would not know if this came from physics in the neutrino sector, or from other relativistic relics; even assuming that such relics do not exist, we would not be able to discriminate between the different cases (shift in temperature, asymmetry or non-thermal distortions). However, we could learn something more from other cosmological probes, such as the study of BBN, leptogenesis and baryogenesis, etc, or from laboratory experiments. For instance, we know from a joint analysis of BBN and neutrino oscillation data that in order to be compatible with measurements of primordial element abundances, the leptonic asymmetry cannot enhance the neutrino density (at CMB and current time) above $N_{\rm eff} \simeq 3.1$ [9].

The CMB is sensitive to $N_{\rm eff}$, first, through the time of equality: when this parameter increases while all other parameters are kept fixed, equality is postponed. However, this effect can be cancelled by increasing simultaneously the matter density by exactly the same amount. Actually, one can also renormalize the cosmological constant in order to preserve all characteristic redshifts in the evolution of the universe (radiation/matter equality, matter/Λ equality). This transformation leaves the CMB almost invariant, but not quite. Indeed, a global

increase of all densities goes with an increase of H_0, which is visible on a small angular scale: it enhances the Silk damping effect (i.e., the effect of diffusion just before photon decoupling, important for $l > 1000$). Generally speaking, a good way to describe the main effect of $N_{\rm eff}$ on the CMB is to say that it changes the scale of Silk damping relative to the scale of the sound horizon at decoupling. Concretely, this will appear as a shift in the damping envelope of high peaks relative to the position of the first peak [1, 50]. This effect is not the only one remaining when all densities are equally enhanced: more neutrinos also imply stronger gravitational interactions between photons and free-streaming species before decoupling. This is especially important for scales that just crossed the Hubble scale during radiation domination. The result is a small shift and damping of the acoustic peak ('baryon drag' effect [1, 51]).

As a result of all these effects, for a minimal 7-parameter model (Λ CDM + $N_{\rm eff}$), the CMB data alone gives $N_{\rm eff} = 3.36^{+0.68}_{-0.64}$ (95%; Planck+WP+highL), well compatible with the standard prediction $N_{\rm eff} = 3.046$. An analysis with a free lensing amplitude A_L of the CMB power spectrum is described in [52].

Like for neutrino masses, data on the cosmological expansion at late time allows a tightening of the bounds on $N_{\rm eff}$, because it removes the partial degeneracy observed in the CMB when all densities are increased in the same proportions. Data on BAO, supernovae or direct measurements of H_0 tighten the constraints on H_0 and/or on the matter density, and forbid an increase in $N_{\rm eff}$ with fixed redshifts for the two equalities (radiation/matter equality, matter/Λ equality). It is worth noticing that unlike models with a free neutrino mass, models with a free $N_{\rm eff}$ have enough freedom for relaxing the tensions between different data sets. For instance, in the ΛCDM + $N_{\rm eff}$ model, the bound on the expansion rate is $H_0 = 69.7^{+5.8}_{-5.3}$ km s^{-1} Mpc^{-1}(95%; Planck+WP), well compatible with $H_0 = 73.8 \pm 4.8$ km s^{-1} Mpc^{-1}(95%; HST) [43]. Even when including BAO data, one gets $H_0 = 69.3^{+3.5}_{-3.4}$ km s^{-1} Mpc^{-1}(95%; Planck+WP+highL +BAO), still compatible with HST measurements.

From the previous discussion on the effect of $N_{\rm eff}$ on the CMB, one can easily infer that there is a positive correlation between measured values of $N_{\rm eff}$ and H_0. Hence, when Planck data is combined with HST data, which favours high values of the expansion rate, one gets more than 2σ evidence for enhanced radiation, $N_{\rm eff} = 3.62^{+0.50}_{-0.48}$ (95%; Planck+WP+highL+HST). Instead, with BAO, the evidence disappears, $N_{\rm eff} = 3.30^{+0.54}_{-0.51}$ (95%; Planck+WP+highL+BAO). Since models with a free $N_{\rm eff}$ relax the tension between the different data sets, it makes sense to combine CMB data with BAO and HST at the same time, which gives $N_{\rm eff} = 3.52^{+0.48}_{-0.45}$ (95%; Planck+WP+highL+BAO+HST), slightly more than 2σ evidence for enhanced radiation (see also [53]).

The conclusion is that if HST data are robust, then one should consider seriously the possibility that $N_{\rm eff}$ exceeds the standard value, because this is one of the simplest ways to relax the constraint between HST and other data sets[6]. This excess could be caused by several effects (leptonic asymmetry, non-standard neutrino phase space distribution, or any type of relativistic relics). If instead we assume that HST results are biased by systematics and should not be included, then the evidence for $N_{\rm eff} > 3.046$ becomes very weak (although a high tensor-to-

[6] Another way is to assume phantom dark energy with $w < -1$ [54], which is much more difficult to motivate on a theoretical basis.

scalar ratio, like the one suggested by the very recent BICEP2 results [55], also tends to slightly favour an excess in $N_{\rm eff}$ [56]).

7.2. Non-standard interactions

Non-standard neutrino interactions (beyond the weak force) could occur in many extensions of the standard model, and could affect cosmological observables in several different ways. For instance, if non-standard neutrino-electron interactions exist, it was shown that they could enhance $N_{\rm eff}$ at most up to 3.1 [57]. Many other cases have been studied in the literature (see the list of references in section 5.3.4 of [1]), still not covering all possibilities. A few representative cases have been studied recently in [58], with two different assumptions concerning the type of self-interaction experienced in the neutrino sector. When the self-interaction is very efficient, neutrinos tend to behave like a relativistic fluid, instead of free-streaming particles with anisotropic stress. Strongly interacting neutrinos with vanishing anisotropic stress are ruled out by Planck data with huge significance. The best fit occurs for standard decoupled neutrinos, and the limits found by [58] on the self-interaction cross-section are very stringent.

7.3. Sterile neutrinos

There are lots of good reasons to postulate the existence of sterile neutrinos: to explain the origin of neutrino masses, the existence of neutrino oscillations, or the mechanism responsible for baryogenesis. Sterile neutrinos could also play the role of dark matter. However, the kind of sterile neutrinos that can be probed with CMB and LSS observations are light sterile neutrinos, with a mass in the eV range. These sterile neutrinos are not motivated by fundamental physics issues, but rather by a few anomalies in short baseline neutrino oscillation data (LSND, MiniBooNE, reactor experiments).

Sterile neutrinos can be generated through various mechanisms, including resonant or non-resonant oscillations with the flavour neutrinos produced in the thermal bath. Depending on the active-sterile neutrino mixing angle(s), sterile neutrinos could thermalize or not [59]. When sterile neutrinos are in the relativistic regime, they can be entirely described in terms of an enhanced $N_{\rm eff}$ (close to four with one generation of thermalized sterile neutrinos). When they become non-relativistic, the parameterization of the model is no longer trivial: in principle, one should specify the phase-space distribution of the sterile neutrino, and vary as many mass parameters as there are neutrino species ($3 + 1$ in the simplest scenarios). Since sterile neutrinos have a significant mass, different models with the same ($N_{\rm eff}$, M_ν) parameters but with different mass splittings and/or a different phase space distribution for the relic sterile neutrino can have distinct signatures on the CMB.

The Planck collaboration has released results for the simple case of two active neutrinos with negligible mass, plus one active neutrino with $m = 0.06$ eV, plus finally one sterile neutrino with a mass m_s and a phase-space distribution equal to the one of active neutrinos multiplied by a suppression factor χ_s. This corresponds to the so-called Dodelson–Widrow (DW) scenario [60], in which sterile neutrinos are generated through non-resonant oscillations. This case can be remapped into the one of thermally distributed sterile neutrinos with a smaller temperature than active neutrinos. The analysis could be carried out in terms of two free parameters ($N_{\rm eff}$, m_s), but it is more convenient to use ($N_{\rm eff}$, ω_s), where $\omega_s \equiv \Omega_s h^2$ is the relic density of sterile neutrinos. Indeed, ω_s is the parameter really probed by the CMB through the lensing and shift-

in-the-peak effects. The Planck paper reports constraints on the quantity 94.1 ω_s eV, called the effective sterile neutrino mass, because it would coincide with the real mass if the sterile neutrino distribution was the same as for active neutrinos in the instantaneous decoupling limit. [41] provides joint constraints on ($N_{\rm eff}$, 94.1 ω_s eV) from CMB+BAO data, showing that a thermalized neutrino with the same temperature as active neutrinos could have a mass of at most half an electron-volt, while a DW neutrino with 1 eV mass should have $\chi_s < 0.5$. The results show no evidence at all for sterile neutrinos.

In the previous sections, we have seen that CMB anisotropy data alone prefers a vanishing neutrino mass, and is well compatible with the standard prediction $N_{\rm eff} = 3.046$. Instead, HST data pushes for extra radiation, while lensing extraction and SZ clusters push for a non-zero neutrino mass. When all these data are considered at the same time, one gets marginal evidence for both $N_{\rm eff} > 3$ and $M_\nu > 0$, which could be interpreted in terms of light sterile neutrinos. [56, 61, 62] performed a joint analysis of all these data sets for a model with three active neutrinos of negligible mass, and one massive DW sterile neutrino. They find marginal evidence for such a sterile neutrino, with a mass in the range $m_s = 0.59 \pm 0.38$ eV (95% C.L.) and with $\chi_s = 0.61 \pm 0.60$ (95% C.L.). These results are in moderate tension with the 3 + 1 scenario that could explain the short baseline anomaly (see also [63, 64]). Note that these results do not only apply to sterile neutrinos and can be easily transposed to the case of other light massive relics, such as thermalized axions (see e.g. [56, 65, 66]).

8. Sensitivity of future experiments to neutrino parameters

The next releases of the Planck CMB satellite will lead to better bounds on neutrino masses. The forecast presented in [46] predicts a neutrino mass sensitivity of $\sigma\left(M_\nu\right) \sim 0.1$ eV from Planck alone, using full temperature and polarization data, and lensing extraction. However, if the small internal tension between temperature and lensing found in the first release survives in the next ones, the final error bar will remain larger.

Several galaxy surveys with better sensitivity and larger volume are about to release data or have been planned over the next decades, including the baryon oscillation spectroscopic survey (BOSS), the dark energy survey (DES), the large synoptic survey telescope (LSST) or the Euclid satellite. Concerning cosmic shear surveys, spectacular improvements are expected from Pan-STARRS, or the DES, LSST and the Euclid surveys already mentioned above.

In the near future, the prediction of [67] is that the combination of full Planck data with BAO scale information from the full BOSS survey could lower the error down to $\sigma\left(M_\nu\right) \sim 0.06$ eV. In addition, the authors of [68] find that adding Lyman alpha data from BOSS should lead to comparable sensitivities, and even better results might be expected from the addition of galaxy power spectrum data from the same survey.

In [69] it was found that the measurement of the galaxy harmonic power spectrum in seven redshift bins by DES should lead to a sensitivity of $\sigma\left(M_\nu\right) \sim 0.06$ eV when combined with Planck data (without lensing extraction). Similar bounds were derived in [70] for another combination of comparable experiments. This shows that at the horizon of 2015, a total neutrino mass close to $M_\nu \simeq 0.1$ eV could be marginally detected at the 2-σ level by cosmological observations. Because this value coincides with the lowest possible total mass in the inverted

hierarchy scenario, the latter could start to be marginally ruled out in case the data still prefers $M_\nu = 0$.

Many papers studied the sensitivity of Euclid to the total neutrino mass. The conservative analysis of [71], taking into account a theoretical error related to the difficulty to model non-linear effects on small scales, suggests an error of the order of $\sigma\left(M_\nu\right) \sim 0.03$ eV in combination with Planck data. Constraints based on the ground-based LSST should be slightly weaker [72]. Hence, in the early 2020s, we expect that a combination of cosmological data sets could detect the total neutrino mass of the normal hierarchy scenario, $M_\nu \simeq 0.05$ eV, at the 2-σ level. If the total mass is instead close to $M_\nu \simeq 0.1$ eV, it will be detected at the 4-σ level. However, in that case, available experiments would not have enough sensitivity to distinguish between an inverted and normal hierarchy scenario with the same M_ν.

Even more progress could be provided by the promising technique of 21-cm surveys. Instead of mapping the distribution of hydrogen atoms through the absorption rate of photons travelling from quasars, it should be possible to observe directly the photons emitted by these atoms at a wavelength $\lambda \simeq 21$ cm from the transition from one hyperfine level to the other. While travelling towards the observer, these photons are redshifted, and seen with a wavelength indicating the position of the emitting atoms in redshift space. Recent theoretical progress in this field shows that using this technique, future dedicated experiments should be able to map hydrogen and hence baryonic fluctuations at very high redshift (typically $6 < z < 12$), and to probe the matter power spectrum deep inside the matter-dominated regime on linear scales [73, 74]. This field is still in its infancy, and the forecasts presented so far have to be approached with caution, due to the difficulty of making a realistic estimate of systematic errors in future data sets. A sensitivity of $\sigma\left(M_\nu\right) \sim 0.075$ eV for the combination of Planck with the square kilometer array (SKA) project, or $\sigma\left(M_\nu\right) \sim 0.0075$ eV with the fast fourier transform telescope (FFTT), was found in [38]. However, the authors show that such impressive experiments would still fail in discriminating between the NH and IH scenario.

An eventual post-Planck CMB satellite or post-Euclid survey would also have a great potential. The forecast analysis in [75] shows that for a CMB satellite of next generation one could get $\sigma\left(M_\nu\right) \sim 0.03$ eV alone, thanks to a very precise reconstruction of the CMB lensing potential, while [76] discusses the potential of cluster surveys. Finally, the authors of [37] show how far the characteristics of an hypothetical galaxy or cosmic shear survey should be pushed in order to discriminate between two allowed NH and IH scenarios with the same total mass.

In the future, the sensitivity of CMB and LSS experiments to $N_{\rm eff}$ will also increase significantly. [46] find that using lensing extraction, the full Planck can lower the error bar down to $\sigma\left(N_{\rm eff}\right) \sim 0.3$. [77, 78] find that the combination of Planck data with the Euclid galaxy survey or cosmic shear survey would give $\sigma\left(N_{\rm eff}\right) \sim 0.1$. However, [79] claims that the combination of Euclid's galaxy survey, cosmic shear survey and cluster mass function measurement would give $\sigma\left(N_{\rm eff}\right) \sim 0.02$.

9. Conclusions

Neutrinos, despite the weakness of their interactions and their small masses, can play an important role in the cosmology that we have reviewed in this contribution. In addition,

cosmological data can be used to constrain neutrino properties, providing information on these elusive particles that complements the efforts of laboratory experiments. In particular, the data on cosmological observables have been used to bound the radiation content of the Universe via the effective number of neutrinos, including a potential extra contribution from other relativistic particles.

But probably the most important contribution of cosmology to our knowledge of neutrino properties is the information provided on the absolute scale of neutrino masses. We have seen that the analysis of cosmological data can lead to either a bound or a measurement of the sum of neutrino masses, an important result complementary to terrestrial experiments such as tritium beta decay and neutrinoless double beta decay experiments. In the near future, thanks to the data from new cosmological experiments, we could even hope to test the minimal values of neutrino masses guaranteed by the present evidences for flavour neutrino oscillations. For this and many other reasons, we expect that neutrino cosmology will remain an active research field in following years.

Acknowledgments

SP was supported by the Spanish grants FPA2011-22975 and Multidark Consolider CSD2009-00064 (MINECO), and by PROMETEO/2009/091 (Generalitat Valenciana).

References

[1] Lesgourgues J, Mangano G, Miele G and Pastor S 2013 *Neutrino Cosmology* (Cambridge: Cambridge University Press)
[2] Dolgov A D 2002 *Phys. Rep.* **370** 333
[3] Hannestad S 2006 *Ann. Rev. Nucl. Part. Sci* **56** 137
[4] Lesgourgues J and Pastor S 2006 *Phys. Rep.* **429** 307
[5] Hannestad S 2010 *Prog. Part. Nucl. Phys.* **65** 185
[6] Wong Y Y Y 2011 *Ann. Rev. Nucl. Part. Sci.* **61** 69
[7] Archidiacono M, Giusarma E, Hannestad S and Mena O 2013 *Adv. High Energy Phys.* **2013** 191047
[8] Kolb E W and Turner M S 1994 *The Early Universe* (Reading, MA: Addison Wesley)
[9] Mangano G, Miele G, Pastor S, Pisanti O and Sarikas S 2012 *Phys. Lett.* B **708** 1
[10] Dodelson S 2003 *Modern Cosmology* (Edinburgh: Academic Press)
[11] Miele G, Pastor S, Pinto T, Pisanti O and Serpico P D 2005 *Nucl. Phys.* B **729** 221
[12] Beringer J *et al* (Particle Data Group) 2012 *Phys. Rev.* D **86** 010001
[13] Sarkar S 1996 *Rep. Prog. Phys.* **59** 1493
[14] Steigman G 2012 *Adv. High Energy Phys.* **2012** 268321
[15] Iocco F, Mangano G, Miele G, Pisanti O and Serpico P D 2009 *Phys. Rep.* **472** 1
[16] Mangano G and Serpico P D 2011 *Phys. Lett.* B **701** 296
[17] Forero D V, Tórtola M A and Valle J W F 2012 *Phys. Rev.* D **86** 073012
[18] Fogli G L, Lisi E, Marrone A, Montanino A, Palazzo A and Rotunno A M 2012 *Phys. Rev.* D **86** 013012
[19] González-García M C, Maltoni M, Salvado J and Schwetz T 2012 *J. High Energy Phys.* JHEP12(2012)123
[20] Giuliani A and Poves A 2012 *Adv. High Energy Phys.* **2012** 857016
[21] Drexlin G, Hannen V, Mertens S and Weinheimer C 2013 *Adv. High Energy Phys.* **2013** 293986
[22] Fogli G L, Lisi E, Marrone A and Palazzo A 2006 *Prog. Part. Nucl. Phys.* **57** 742

[23] Fogli G L, Lisi E, Marrone A, Melchiorri A, Palazzo A, Rotunno A M, Serra P and Silk J 2008 *Phys. Rev.* D **78** 033010
[24] González-García M C, Maltoni M and Salvado J 2010 *J. High Energy Phys.* JHEP08(2010)117
[25] Primack J R 2011 arXiv:astro-ph/0112336
[26] Boyarsky A, Ruchayskiy O and Shaposhnikov M 2009 *Ann. Rev. Nucl. Part. Sci.* **59** 191
[27] Hu W, Eisenstein D J and Tegmark M 1998 *Phys. Rev. Lett.* **80** 5255
[28] Lewis A, Challinor A and Lasenby A 2000 *Astrophys.* J. **538** 473
[29] Lesgourgues J and Tram T 2011 *J. Cosmol. Astropart. Phys.* JCAP09(2011)032
[30] Brandbyge J and Hannestad S 2010 *J. Cosmol. Astropart. Phys.* JCAP01(2010)021
[31] Bird S, Viel M and Haehnelt M G 2012 *Mon. Not. R. Astron. Soc* **420** 2551
[32] Wagner C, Verde L and Jimenez R 2012 *Astrophys.* J. **752** L31
[33] Villaescusa-Navarro F, Marulli F, Viel M, Branchini E, Castorina E, Sefusatti E and Saito S 2014 *J. Cosmol. Astropart. Phys.* JCAP03(2014)011
[34] Castorina E, Sefusatti E, Sheth R K, Villaescusa-Navarro F and Viel M 2014 *J. Cosmol. Astropart. Phys.* JCAP02(2014)049
[35] Costanzi M, Villaescusa-Navarro F, Viel M, Xia J Q, Borgani S, Castorina E and Sefusatti E 2013 *J. Cosmol. Astropart. Phys.* JCAP12(2013)012
[36] Lesgourgues J, Pastor S and Perotto L 2004 *Phys. Rev.* D **70** 045016
[37] Jimenez R, Kitching T, Peña-Garay C and Verde L 2010 *J. Cosmol. Astropart. Phys.* JCAP05(2010)035
[38] Pritchard J R and Pierpaoli E 2008 *Phys. Rev.* D **78** 065009
[39] Hou Z *et al* 2014 *Astrophys. J.* **782** 74
[40] Ade P A R *et al* (Planck Collaboration) 2013 arXiv:1303.5062
[41] Ade P A R *et al* (Planck Collaboration) 2013 arXiv:1303.5076
[42] Hinshaw G *et al* (WMAP Collaboration) 2013 *Astrophys. J. Suppl.* **208** 19
[43] Riess A G *et al* 2011 *Astrophys. J.* **730** 119
Riess A G *et al* 2011 *Astrophys. J.* **732** 129 (erratum)
[44] Marra V, Amendola L, Sawicki I and Valkenburg W 2013 *Phys. Rev. Lett.* **110** 241305
[45] Ade P A R *et al* (Planck Collaboration) 2013 arXiv:1303.5077
[46] Perotto L, Lesgourgues J, Hannestad S, Tu H and Wong Y Y Y 2006 *J. Cosmol. Astropart. Phys.* JCAP10 (2006)013
[47] Ade P A R *et al* (Planck Collaboration) 2013 arXiv:1303.5080
[48] Battye R A and Moss A 2014 *Phys. Rev. Lett.* **112** 051303
[49] Beutler F *et al* (BOSS Collaboration) 2014 arXiv:1403.4599
[50] Hou Z, Keisler R, Knox L, Millea M and Reichardt C 2013 *Phys. Rev.* D **87** 083008
[51] Bashinsky S and Seljak U 2004 *Phys. Rev.* D **69** 083002
[52] Said N, di Valentino E and Gerbino M 2013 *Phys. Rev.* D **88** 023513
[53] Zheng W, Li H, Xia J Q, Wan Y P, Li S Y and Li M 2014 *Int. J. Mod. Phys.* D **23** 1450051
[54] Cheng C and Huang Q G 2014 *Phys. Rev.* D **89** 043003
[55] Ade P A R *et al* (BICEP2 Collaboration) 2014 arXiv:1403.3985
[56] Giusarma E, Di Valentino E, Lattanzi M, Melchiorri A and Mena O 2014 arXiv:1403.4852
[57] Miele G, Pastor S, Pinto T, Pisanti O and Serpico P D 2006 *Nucl. Phys.* B **756** 100
[58] Archidiacono M and Hannestad S 2013 arXiv:1311.3873
[59] Mirizzi A, Mangano G, Saviano N, Borriello E, Giunti C, Miele G and Pisanti O 2013 *Phys. Lett.* B **726** 8
[60] Dodelson S and Widrow L M 1994 *Phys. Rev. Lett.* **72** 17
[61] Wyman M, Rudd D H, Vanderveld R A and Hu W 2014 *Phys. Rev. Lett.* **112** 051302
[62] Hamann J and Hasenkamp J 2013 *J. Cosmol. Astropart. Phys.* JCAP10(2013)044
[63] Hamann J, Hannestad S, Raffelt G G and Wong Y Y Y 2011 *J. Cosmol. Astropart. Phys.* JCAP09(2011)034
[64] Gariazzo S, Giunti C and Laveder M 2013 *J. High Energy Phys.* JHEP11(2013)211
[65] Raffelt G G, Hamann J, Hannestad S, Mirizzi A and Wong Y Y Y 2010 *AIP Conf. Proc.* **1274** 66

[66] Archidiacono M, Hannestad S, Mirizzi A, Raffelt G G and Wong Y Y Y 2013 *J. Cosmol. Astropart. Phys.* JCAP10(2013)020
[67] Sekiguchi T, Ichikawa K, Takahashi T and Greenhill L 2010 *J. Cosmol. Astropart. Phys.* JCAP03(2010)015
[68] Gratton S, Lewis A and Efstathiou G 2008 *Phys. Rev.* D **77** 083507
[69] Lahav O, Kiakotou A, Abdalla F B and Blake C 2010 *Mon. Not. R. Astron. Soc.* **405** 168
[70] Namikawa T, Saito S and Taruya A 2010 *J. Cosmol. Astropart. Phys.* JCAP12(2010)027
[71] Audren B, Lesgourgues J, Bird S, Haehnelt M G and Viel M 2013 *J. Cosmol. Astropart. Phys.* JCAP01 (2013)026
[72] Hannestad S, Tu H and Wong Y Y Y 2006 *J. Cosmol. Astropart. Phys.* JCAP06(2006)025
[73] Pritchard J R and Loeb A 2012 *Rep. Prog. Phys.* **75** 086901
[74] Shimabukuro H, Ichiki K, Inoue S and Yokoyama S 2014 arXiv:1403.1605
[75] Lesgourgues L, Perotto L, Pastor S and Piat M 2006 *Phys. Rev.* D **73** 045021
[76] Wang S, Haiman Z, Hu W, Khoury J and May M 2005 *Phys. Rev. Lett.* **95** 011302
[77] Kitching T D, Heavens A F, Verde L, Serra P and Melchiorri A 2008 *Phys. Rev.* D **77** 103008
[78] Carbone C, Verde L, Wang Y and Cimatti A 2011 *J. Cosmol. Astropart. Phys.* JCAP03(2011)030
[79] Basse T, Bjaelde O E, Hamann J, Hannestad S and Wong Y Y Y 2013 arXiv:1304.2321